

# Tropical Meteorology

Kerry Emanuel  
Program in Atmospheres, Oceans, and Climate  
Massachusetts Institute of Technology  
Cambridge, MA 02139, USA

October 5, 1999

# Introduction

## 1 Radiative-Convective Equilibrium

We begin with a discussion of the physics underlying the normal state of the tropical atmosphere. The average vertical thermal structure of the atmosphere is illustrated in Figure 1.1. The lowest layer, the troposphere, extends from the surface upward to 8-15 km, depending mostly on the latitude and season. It is characterized by temperature decreasing with altitude, at an average rate of about  $6\text{ K km}^{-1}$ . This upward decrease of temperature ends, often abruptly, at the tropopause, above which the temperature is constant or increases with altitude. This layer is called the stratosphere. At an altitude of between 40 and 50 km., the temperature lapse rate again changes sign, at the stratopause, and in the mesosphere the temperature decreases upward. Above the mesopause lies the thermosphere, in which the temperature once again increases with altitude, and here the mean free path between molecular collisions becomes appreciable. The high temperatures of the upper thermosphere are caused by collisions between atmospheric constituents and high energy particles originating in the solar wind; the actual temperature of this region is a strong function of the level of solar substorm activity. But below the thermosphere, the temperature is determined by transfer of electromagnetic radiation, and in the troposphere convective heat transfer is important as well.

### 1.1 General principles of radiative transfer

The two major constituents of the atmosphere, molecular oxygen and nitrogen, are very nearly transparent to both solar and terrestrial radiation, although some scattering of solar radiation does occur. Oxygen and nitrogen are diatomic molecules with a very limited number of degrees of freedom, thus they are poor absorbers of radiation. If these were the only gases in the atmosphere, then it would be almost completely transparent and the earth's surface would radiate at very nearly the black body temperature necessary to balance the input of solar radiation. One can calculate what this temperature would be. At the mean radius of the earth's orbit about the sun, the flux of solar radiation,  $S_0$ , is known as the *solar constant* and has a value of about  $1367\text{ W m}^{-2}$ . By elementary geometry, the amount of this radiation intercepted by the earth, per unit surface area of the earth, is just  $S_0/4$ . A fraction of this radiation,  $\alpha_p$  is reflected back to space by the earth's surface and by clouds; this fraction is known as the *planetary albedo*. By the Stefan-Boltzmann law, the black body temperature is given by

$$\sigma T^4 = \frac{S_0}{4}(1 - \alpha_p), \quad (1.1)$$

where  $\sigma$  is  $5.67 \times 10^{-8}\text{ W m}^{-2}\text{K}^{-4}$ . Using a planetary albedo of 0.3, this gives a black body temperature of 255 K or -18 C, very much colder than the average surface temperature of the earth, which is 288 K or 15 C.

The surface temperature of the earth is higher than its black body temperature owing to the presence of a few principally triatomic species, notably water vapor, carbon dioxide and ozone. While these represent very small fractions of the atmosphere by mass, they are critical absorbers and emitters of radiation, because their structure allows for many more degrees of freedom; especially in rotation and vibration. Condensed water, in the form of clouds, is also very important in reflecting, absorbing and emitting radiation.

Figure 1.2 shows two black body curves, for the sun and earth, respectively, as well as atmospheric absorption characteristics near the surface and near 11 km. First note that, because the earth's effective emitting temperature is about 255 K whereas that of the sun is close to 6000 K, their two spectra have

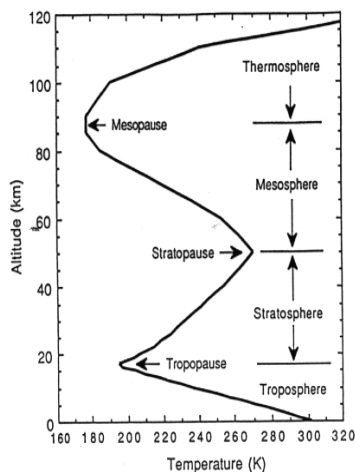


Figure 1.1: The main zones of the atmosphere defined according to a standard atmosphere at 15°N. Data taken from U.S. Standard Atmosphere Supplements (1966)

almost no overlap. So we may usefully talk about solar and terrestrial radiation, or shortwave and longwave radiation, without ambiguity. Also note that the solar spectrum peaks in a region in which there is very little atmospheric absorption, so that most sunlight that is not reflected or absorbed by clouds reaches the surface. Virtually all of the very high energy, ultraviolet radiation is absorbed in the middle stratosphere in a photochemical reaction in which molecular oxygen breaks into 2 oxygen atoms, some of which combine with other available oxygen atoms to form ozone ( $O_3$ ). Once formed, ozone itself absorbs some ultraviolet radiation. Were most of the incoming ultraviolet spectrum to reach the surface, life as we know it would not be possible. The high temperatures of the upper stratosphere are owing to the absorption of ultraviolet radiation by ozone.

In the terrestrial spectrum, there are large numbers of absorption lines (which are broadened by both Doppler and pressure effects), owing mostly to the triatomic molecules water vapor and carbon dioxide, but with some notable contributions from other trace species such as methane. Water vapor content decreases sharply with height, but there are still large water absorption effects at 11 km. Taken together, the relative opacity of the atmosphere to terrestrial radiation makes for a strong “greenhouse effect”.

## 1.2 Simple models without phase change

### 1.2.1 Pure radiative equilibrium

We begin with a very simple model of pure radiative equilibrium, as illustrated by Figure 1.3. In the first instance, consider 2 layers of gas each with an emissivity of unity in the terrestrial band but which are completely transparent to solar radiation. They overly a surface of emissivity unity. In radiative equilibrium, each layer emits upward and downward, and the surface emits upward. The energy balance for the upper

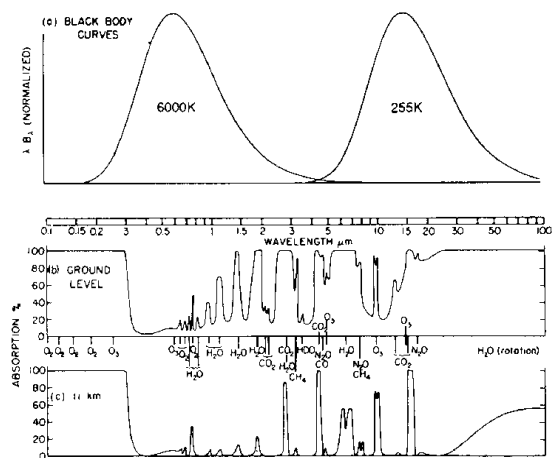


Figure 1.2: The normalized blackbody emission spectra for the sun (6000 k) and Earth (255 K) as a function of wavelength (top). The fraction of radiation absorbed in passing between the surface and the top of the atmosphere (middle). The fraction of radiation absorbed in passing between the tropopause and the top of the atmosphere (bottom). The atmospheric molecules contributing the important absorption features at each frequency are noted. From Goody and Yung (1989).

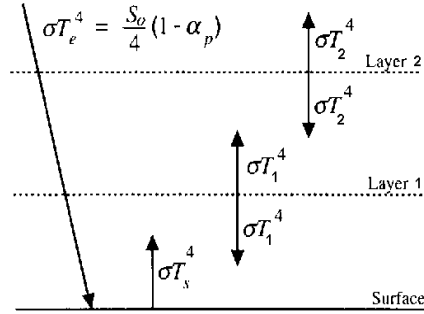


Figure 1.3: **Simple radiative equilibrium model.** The surface receives solar radiation and emits infrared radiation upward. The atmosphere consists of two layers of longwave emissivity unity and shortwave absorptivity zero.

layer is

$$2\sigma T_2^4 = \sigma T_1^4, \quad (1.2)$$

where  $T_2$  is the temperature of the upper layer and  $T_1$  is the temperature of the lower layer. Likewise, the energy balance of the lower layer is given by

$$2\sigma T_1^4 = \sigma T_s^4 + \sigma T_2^4, \quad (1.3)$$

where  $T_s$  is the surface temperature. The surface energy balance is simply

$$\sigma T_s^4 = \sigma T_e^4 + \sigma T_1^4, \quad (1.4)$$

where  $T_e$  is the effective blackbody emission temperature, defined

$$\sigma T_e^4 = \frac{S_o}{4}(1 - \alpha_p).$$

Now we may solve (1.2) - (1.4) for the three temperatures, giving

$$T_2 = T_e = 255 \text{ K},$$

$$T_1 = 2^{\frac{1}{4}} T_e = 303 \text{ K}, \quad (1.5)$$

$$T_s = 3^{\frac{1}{4}} T_e = 336 \text{ K}.$$

The surface temperature is substantially greater than the blackbody equilibrium temperature. Note also that since  $T_1 > T_e$ , the surface actually received more radiation from the atmosphere than it does from the sun. More to the point, we can show that the air in immediate contact with the ground is not in thermal

equilibrium with the ground. We can do this by inserting a vanishingly thin layer of air between the surface and the first, opaque layer. This thin layer has vanishing emissivity,  $\varepsilon$ , and its energy balance is

$$2\varepsilon\sigma T_a^4 = \varepsilon\sigma T_s^4 + \varepsilon\sigma T_1^4, \quad (1.6)$$

where  $T_a$  is the temperature of the thin layer next to the surface. Since the layer is vanishingly thin, it does not affect the energy balance of the surface and other layers. The solution to (1.6) is then

$$T_a = \left(\frac{5}{2}\right)^{\frac{1}{4}} T_e = 321 \text{ K}. \quad (1.7)$$

So clearly, in radiative equilibrium, the surface air is not in thermal equilibrium with the surface. This creates the potential for *convective* heat transport away from the surface. This will be the subject of the next section.

### 1.2.2 Radiative-convective equilibrium

In the previous subsection, we noted that the radiative equilibrium distribution in a simple model gives thermal disequilibrium between the surface and the immediate overlying atmosphere, implying that some convective heat transport will occur. In fact, the entire atmosphere shown in Figure 1.2 must convect, because it's vertical temperature distribution is unstable. Suppose we take a test sample from the lower layer in Figure 1.2 and lift it by a *reversible adiabatic* process up to the middle of the upper layer. If the density of the lifted sample is less than that of the surrounding air, then buoyancy will accelerate it upward, in the same direction as the original displacement. If an adiabatic displacement in an equilibrium system results in a force in the same direction as the displacement, that displacement is unstable. Let's calculate the specific volume (or inverse density) of the adiabatically displaced test sample and compare it to the specific volume of the upper layer. If the sample has a greater specific volume, its density will be less and the displacement will thus be unstable.

The specific volume of the sample, if it does not undergo phase changes, may be expressed as a function of any two other state variables. Since entropy is conserved in a reversible adiabatic displacement, it makes a convenient variable to work with. Thus we express the specific volume,  $\alpha$ , as

$$\alpha = \alpha(p, s),$$

where  $s$  is the specific entropy and  $p$  is the pressure. Now we are comparing the specific volume of the displaced sample to that of its surroundings *at the same pressure*. So we can write the difference, if it is small, as

$$\alpha_p - \alpha \simeq \left(\frac{\partial\alpha}{\partial s}\right)_p (s_p - s). \quad (1.8)$$

The partial derivative in (1.8) is taken at constant pressure. We can now use one of *Maxwell's relations*, which can be derived from the First Law of Thermodynamics:

$$\left(\frac{\partial\alpha}{\partial s}\right)_p = \left(\frac{\partial T}{\partial p}\right)_s. \quad (1.9)$$

Using (1.9) in (1.8) gives

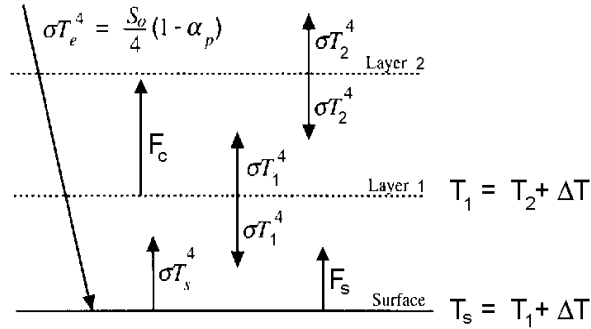


Figure 1.4: **Addition of convective fluxes,  $F_s$  and  $F_c$  to the simple equilibrium model.**

$$\alpha_p - \alpha \simeq \left( \frac{\partial T}{\partial p} \right)_s (s_p - s). \quad (1.10)$$

Since the *adiabatic lapse rate*,  $\left( \frac{\partial T}{\partial p} \right)_s$ , is always positive, (1.10) shows that the atmosphere will be unstable if its entropy decreases upward, so that the sample displaced from the lower to the upper layer will have an entropy that is greater than that of the upper layer. *The condition for convective instability is simply that the entropy of the gas decreases upward along the gravitational vector.*

As it turns out, the radiative equilibrium entropy distribution is unstable in the earth's troposphere. For this reason, much of the troposphere is convecting; in fact, this is a good definition of the tropical troposphere. But convection is a relatively fast process in the atmosphere, with characteristic time scales of a few hours. On the other hand, perturbations away from radiative equilibrium decay back to equilibrium on time scales closer to 40 days. Therefore, in a competition between the two processes, convection must “win” in the sense that the observed temperature distribution will be much closer to convective than to radiative equilibrium.

Atmospheres in which the heat transport by radiation and convection are in balance are said to be in *radiative-convective equilibrium*. As a first cut at calculating a radiative-convective equilibrium state, we can suppose that the effect of convection is to fix the temperature difference between the upper and lower layers of our simple model at a value of  $\Delta T$ . Figure 1.4 shows our simple radiative-convective equilibrium model. We suppose that, in addition to the radiative fluxes, a convective heat flux,  $F_c$ , carries heat from the lower to the upper layer, and a turbulent heat flux,  $F_s$ , also carries heat from the surface into the lower layer. The energy balances are

Surface:

$$F_s + \sigma T_s^4 = \sigma T_e^4 + \sigma T_1^4. \quad (1.11)$$

Lower layer:

$$2\sigma T_1^4 + F_c = \sigma T_s^4 + \sigma T_2^4 + F_s. \quad (1.12)$$

Upper layer:

$$2\sigma T_2^4 = \sigma T_1^4 + F_c. \quad (1.13)$$

We next *impose* a condition for convective neutrality:

$$T_1 = T_2 + \Delta T, \quad (1.14)$$

and

$$T_s = T_2 + 2\Delta T. \quad (1.15)$$

Solving (1.11) - (1.15) for the various quantities gives the following solution:

$$T_2 = T_e,$$

$$T_1 = T_e + \Delta T,$$

$$T_s = T_e + 2\Delta T,$$

$$F_s = \sigma T_e^4 \left[ 1 + (1+x)^4 - (1+2x)^4 \right],$$

and

$$F_c = \sigma T_e^4 \left[ 2 - (1+x)^4 \right],$$

where  $x \equiv \Delta T/T_e$ . The condition for the viability of this solution is that  $F_s$  and  $F_c$  are positive. Given that  $\Delta T$  is positive, both of the convective fluxes will be positive if and only if  $x < 0.1404$ . Also, we can see that the smaller the adiabatic lapse rate, to which  $x$  is proportional, the greater the convective heat fluxes must be.

### 1.3 General principles of moist convection

In the earth's atmosphere, the actual radiative-convective equilibrium state is far more complex than is captured by these simple models. For one thing, the emissivity of each infinitesimal layer is a strong function of the concentration of absorbing gases and clouds, and the principal absorbers, water vapor and clouds, are strong functions of the convection, which is part of the response of the system. Secondly, the convection that actually occurs is *moist convection*, in the form of cumulus and cumulonimbus clouds, so, among other things, we have to redefine entropy and density to take into account the presence of water substance.

One fundamental aspect of radiative-convective equilibrium remains true in the moist case: The convective time scale is much shorter than the radiative time scale, so the actual state of the atmosphere remains very close to one of neutrality to convection. Unfortunately, the state of neutrality to moist convection contains several ambiguities that prevent an exact calculation, but a good approximation to the actual vertical temperature structure of the tropical atmosphere is that it is neutral to the reversible ascent of air (without considering the ice phase) from the boundary layer. To be more precise, the density of the tropical atmosphere at any pressure level is very nearly equal to the density of air that has been lifted reversibly from the well-mixed portion of the subcloud layer.



Since water changes phase and can constitute up to 4% of the mass of a sample of air in the Tropics, we must consider the variable water content of the air in defining its density (or specific volume). One can assume that all the condensed water in a sample is falling at very nearly its terminal velocity, so that the effective specific volume of a sample containing a mixture of dry air, water vapor and condensed water is given by

$$\alpha = \frac{V_a + V_c}{M_d + M_v + M_c}, \quad (1.16)$$

where  $V_a$  is the volume occupied by air,  $V_c$  is the volume occupied by condensate,  $M_d$  is the mass of dry air in the sample,  $M_v$  is the mass of water vapor, and  $M_c$  is the mass of condensate. Using the ideal gas law,

$$pV = nR^*T,$$

the volume occupied by air is given by

$$V_a = \frac{R^*T}{p} \left( \frac{M_d}{m_d} + \frac{M_v}{m_v} \right) = \frac{R_d T}{p} (M_d + M_v/\epsilon). \quad (1.17)$$

Here  $R^*$  is the universal gas constant,  $n$  is the number of moles of gas,  $m_d$  and  $m_v$  are the mean molecular weight of dry air and of water vapor, respectively,  $\epsilon$  is defined as  $m_v/m_d$ , and  $R_d$  is defined as  $R^*/m_d$ . Using (1.17) in (1.16) gives

$$\alpha = \frac{R_d T}{p} (1 - q_t + q/\epsilon) \left( 1 + \frac{q_c}{1 - q_c} \frac{\rho_a}{\rho_c} \right). \quad (1.18)$$

Here  $q_t$  is the *total water content* (the mass of water substance divided by the total mass of the sample),  $q$  is the *specific humidity* (the mass of water vapor divided by the mass of the sample),  $q_c$  is the mass of condensate per unit mass of the sample, and  $\rho_a$  and  $\rho_c$  are respectively the densities of air and condensed water. Since both  $q_c$  and  $\frac{\rho_a}{\rho_c}$  are of order  $10^{-3}$  in the atmosphere, we can safely neglect the last term in parentheses on the right, so that to an excellent approximation,

$$\alpha = \frac{R_d T}{p} (1 - q_t + q/\epsilon). \quad (1.19)$$

It is convenient to use (1.19) to define a quantity called the *density temperature*,  $T_{rho}$ , which is the temperature dry air would have to have to give the same density as a moist sample at the same temperature and pressure:

$$T_\rho \equiv T (1 - q_t + q/\epsilon). \quad (1.20)$$

Since  $\epsilon \simeq 0.622$ , a moist sample without condensate is always less dense than a dry sample at the same temperature and pressure and thus will have a higher density temperature. But condensate increases the effective density temperature and, in a cloud, can easily overcome the effect of water vapor.

Since, in a moist atmosphere, density is a function of not just two, but three other state variables (say, entropy, pressure and total water content), it is not possible to derive a simple temperature-pressure relationship that defines the state of convective neutrality, as in the dry case. Even more importantly, moist convection involves only a tiny fraction of the atmosphere in turbulent convective motions at any given time; the rest of the atmosphere is quiescent. Nonetheless, as we shall illustrate presently, much of the tropical

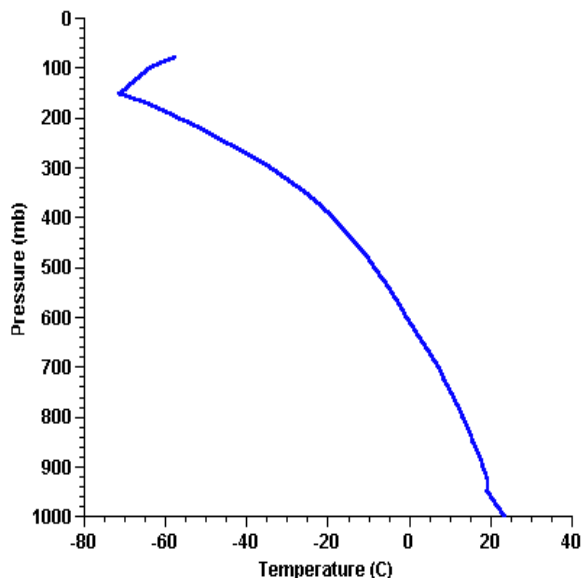


Figure 1.5: Temperature profile averaged over several thousand tropical soundings.

atmosphere turns out to be such that air from close to the surface, when lifted adiabatically and reversibly, is very nearly neutrally buoyant. To calculate its buoyancy, we compare its density temperature to that of the surrounding atmosphere.

To calculate the density temperature of a lifted parcel, we must know its temperature, specific humidity and total water content at each pressure level. In a reversible process, the total water content is conserved and is therefore equal to its starting value. The temperature may be calculated from the conservation of entropy in a reversible adiabatic process. In a sample containing a mixture of dry air, water vapor and condensed water, the specific enthalpy is given by (see Emanuel, 1994)

$$s = (c_{pd}(1 - q_t) + c_l q_t) \ln(T) - R_d \ln(p_d) + \frac{L_v q}{T} - q R_v \ln(\mathcal{H}), \quad (1.21)$$

where  $c_{pd}$  is the heat capacity at constant pressure of dry air,  $c_l$  is the heat capacity of liquid water,  $p_d$  is the partial pressure of dry air,  $L_v$  is the (temperature dependent) latent heat of vaporization,  $R_v$  is the gas constant for water vapor, and  $\mathcal{H}$  is the relative humidity. Fortunately, we can safely assume that, in clouds, the liquid and vapor phases of water are in thermodynamic equilibrium, so that in that case  $\mathcal{H} = 1$  and the specific humidity,  $q$  is given by its saturation value ( $q^*$ ), which is just a function of pressure and temperature. Thus we may use the conservation of  $q_t$  and  $s$ , as given by (1.21), to calculate the temperature (and therefore  $q^*$ ) at each pressure level within a cloud created by reversible adiabatic ascent.

Figure 1.5 shows an example of the vertical profile of temperature of air lifted from near the surface in typical tropical conditions. Note that the lapse rate (called the *moist adiabatic lapse rate*) increases in magnitude with height and asymptotically approaches the dry adiabatic lapse rate at low temperature. This reflects the fact that as the air rises and water vapor condenses into liquid water, latent heat is released, thus preventing the air from cooling as rapidly as the dry adiabatic rate. But as the air continues to ascend, less and less water condenses, and the lapse rate becomes more nearly dry adiabatic.

Thus an important effect of moist convection is to reduce the temperature lapse rate of the lower troposphere.

#### 1.4 Simple models incorporating the effects of phase change

A crude account of the effects of moist convection on radiative-convective equilibrium can be made by taking the model of section 1.2.2 and allowing the temperature lapse rate to be variable. We also now have to interpret the turbulent fluxes,  $F_s$  and  $F_c$ , as turbulent fluxes of enthalpy,  $k$ , defined

$$k \equiv c_p T + L_v q.$$

Thus we start with ((1.11))-((1.13)) but we replace ((1.14)) and ((1.15)) with

$$T_1 = T_2 + \Delta T_2, \tag{1.22}$$

and

$$T_s = T_1 + \Delta T_1, \tag{1.23}$$

where we suppose that moist convection imposes  $\Delta T_1 < \Delta T_2$ . Once again we find that  $T_2 = T_e$ , so that

$$T_1 = T_e + \Delta T_2, \tag{1.24}$$

and

$$T_s = T_e + \Delta T_1 + \Delta T_2. \tag{1.25}$$

*The most obvious, and in some ways the most important effect of moist convection is to cool the surface, since the warmer the atmosphere, the more moisture it contains and the smaller  $\Delta T_1$  is relative to  $\Delta T_2$ .*

We can also solve for the turbulent enthalpy fluxes:

$$F_s = \sigma T_e^4 \left[ 1 + (1 + x_2)^4 - (1 + x_1 + x_2)^4 \right], \tag{1.26}$$

and

$$F_c = \sigma T_e^4 \left[ 2 - (1 + x_2)^4 \right], \tag{1.27}$$

where  $x_1 \equiv \Delta T_1/T_e$  and  $x_2 \equiv \Delta T_2/T_e$ . Clearly, in this simple model, moisture has no effect on the net convective enthalpy flux from the lower to the upper layer, but it *increases* the net turbulent enthalpy flux from the surface to the atmosphere. It does this because, by reducing the surface temperature, it reduces the radiative flux away from the surface, thus necessitating an increase in the turbulent flux.

#### 1.5 Quantitative assessments of the equilibrium state - observations

The real world is rendered far more complex than the simple models we have considered here by the fact that the emissivity varies strongly with altitude, water vapor content, and condensed phase water content. Since the emissivity is less than unity, each layer communicates not just with its immediate neighbors, as in our simple model, but with all the other layers as well. Also, the convection transports enthalpy and water not just to adjacent layers but between many possible combinations of layers. Moreover, the water

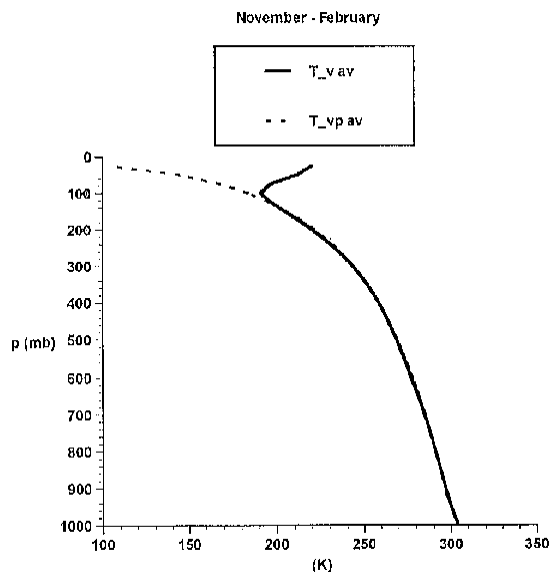


Figure 1.6: **Actual (solid) and moist adiabatic (dashed) density temperature averaged over several thousand tropical soundings.**

content (and thus the emissivity) is determined by the convection, so the radiative-convective problem is highly interactive.

We can test one aspect of our assumptions about the nature of moist radiative-convective equilibrium in a relatively straightforward way. By examining tropical balloon soundings, we can examine the extent to which the tropical atmosphere is close to a state of convective neutrality. Figure 1.6 compares the density temperature of air lifted from the subcloud layer with that of its environment, in a particular sounding. There is a close correspondence. This can be seen in somewhat more detail in Figure 1.7, which shows the average difference between the density temperature of a reversibly lifted parcel and that of its environment, as a function of the pressure level to which the parcel has been lifted, and the pressure level from which it has been lifted. While air lifted from the surface layer (roughly, the first 100 m above the surface) is clearly unstable, air from the interior of the subcloud layer (which usually extends to about 50 mb above the surface) is nearly neutrally buoyant when lifted.

A cartoon of radiative-convective equilibrium is shown in Figure 1.8. Air ascends rapidly within widely-spaced, precipitating convective clouds. The fractional area covered by the deep clouds themselves is so small that their direct affect on radiative transfer is usually very small. (On the other hand, the cirrus anvils associated with the deep clouds can have large effects on both incoming shortwave and on longwave radiation. Lack of understanding of the control of these clouds is a major source of uncertainty in climate prediction.) In compensation for the rapidly ascending air in the tall convective towers, unsaturated air sinks in between the clouds (in space and time). As it does so, it cools by infrared emission to space, at a rate of around  $1 - 2 \text{ K day}^{-1}$ . (Some air also sinks into the subcloud layer in unsaturated downdrafts cooled by the evaporation and melting of precipitation. These downdrafts are of crucial importance in the energy, momentum and water balance of the subcloud layer.) The consequent loss of entropy means that the potential temperature in the tropical atmosphere increases upward, and since the temperature of

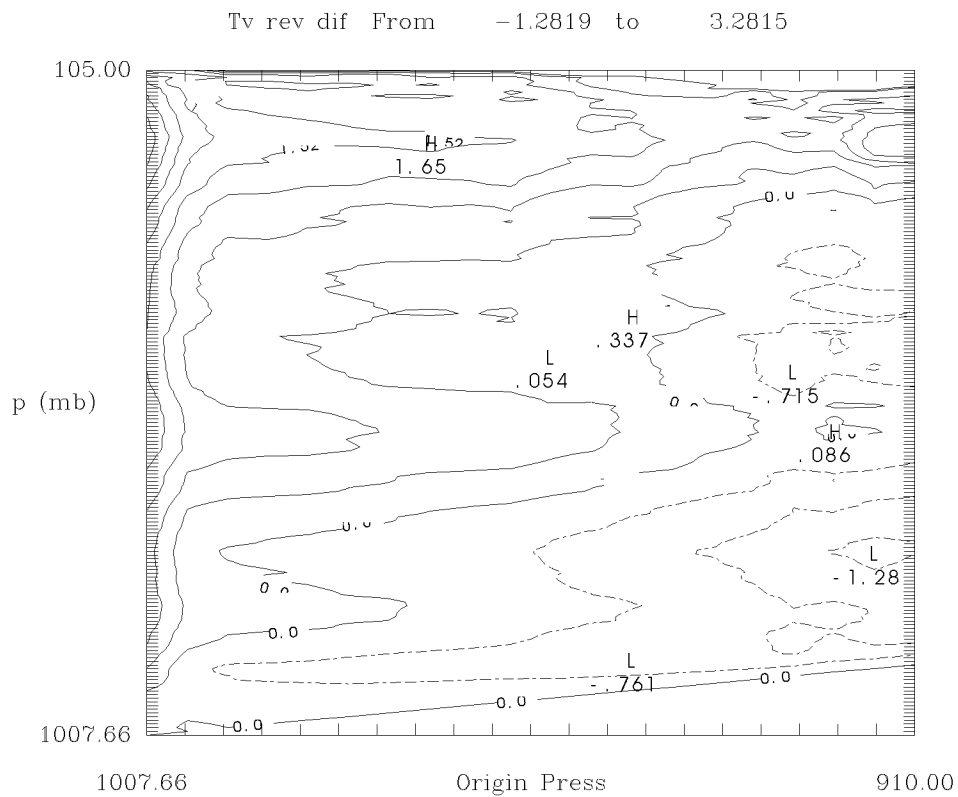


Figure 1.7: Difference between the density temperature of a parcel lifted reversibly from the pressure level indicated on the abscissa and that of its environment, as a function of the pressure level to which the parcel is lifted (ordinate). The quantity has been averaged over several thousand soundings from the equatorial western Pacific region. Ice phase ignored in the calculation of lifted temperature.

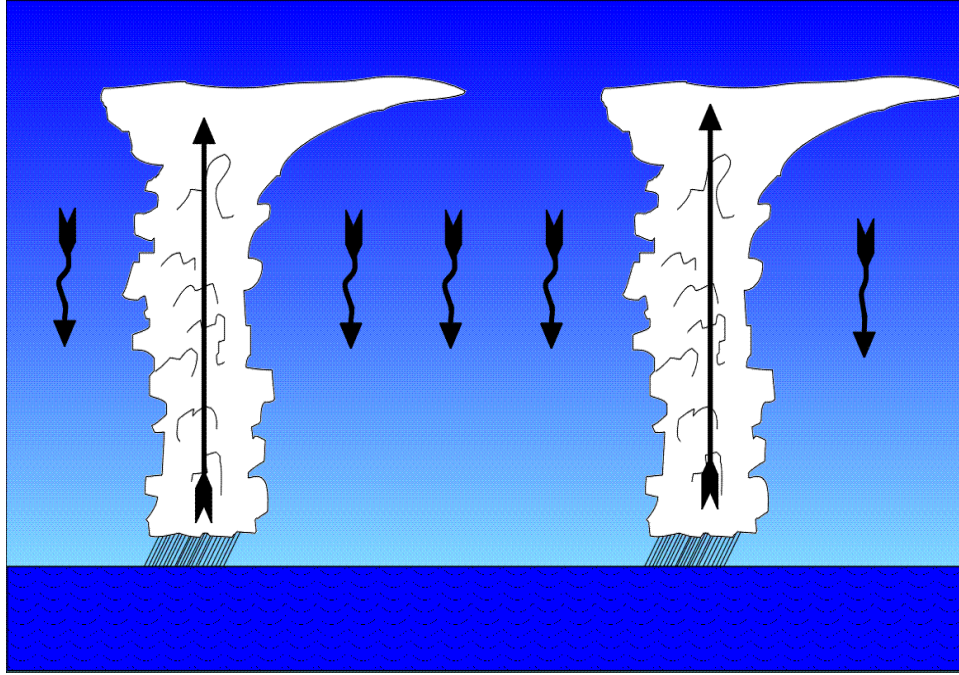


Figure 1.8: Moist radiative-convective equilibrium. Air rises rapidly (typically, a few  $m \bar{s}^{-1}$ ) within clouds, approximately conserving moist static energy. The clouds cover a very small fractional area, so the return flow is weak (roughly  $1 - 2 \text{ cm } \bar{s}^{-1}$ ). The clear, subsiding air loses enthalpy by radiation to space, so that as the air sinks, its potential temperature increases, following approximately a moist adiabat.

the environment is nearly that of the cloud, this upward increase is nearly that along a moist adiabat. (The decided stability of the tropical atmosphere to unsaturated vertical displacements is of considerable importance in the dynamics of the tropical atmosphere.) Were the sinking air between clouds to receive no water, the relative humidity between clouds would be extremely low from just below the tropopause all the way down to the turbulent subcloud layer. While very low humidities are indeed observed from time to time in the tropical upper troposphere, such low humidities are unusual, particularly in the low and middle troposphere. Figure ?? shows a series of histograms of relative humidity in the Tropics. On average, the air subsiding outside of clouds receives water by detrainment from clouds and by evaporation of falling precipitation, so that, on average, the specific humidity increases downward at all altitudes and the relative humidity increases downward in the lower troposphere. The loss of energy in the column by the divergence of the net radiative flux is compensated in equilibrium by the convergence of the turbulent vertical moist static energy flux. The moist static energy,  $h$ , is defined approximately as

$$h \equiv c_p T + L_v q + gz, \quad (1.28)$$

where  $g$  is the acceleration of gravity and  $z$  is altitude. (See Emanuel [4] for an exact definition.) This turbulent energy flux originates as an enthalpy flux away from the sea surface, carried by unsaturated, turbulent eddies in the subcloud layer and is then handed over to a turbulent flux carried by a spectrum of moist convective clouds. (The air within these clouds carries with it approximately the value of  $h$  near cloud

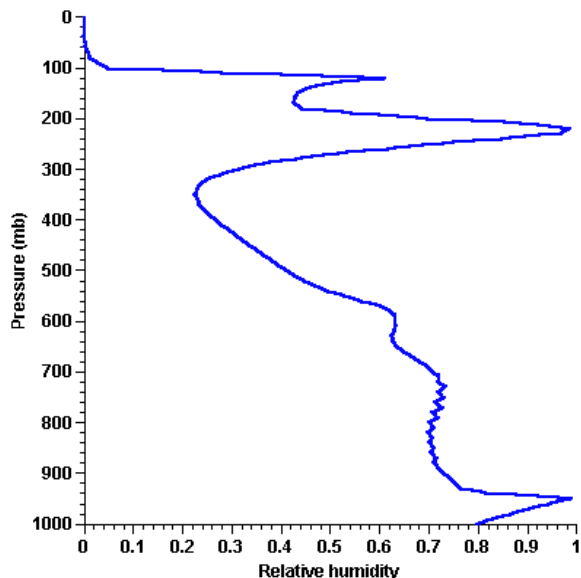


Figure 1.10: Relative humidity profile in radiative-convective equilibrium, using the calibrated convective scheme described by Emanuel and Zivkovic-Rothman [6].

base; this is somewhat larger than the value of  $h$  in the environment of the clouds, so the turbulent flux of  $h$  is upward.) One consequence of this balance is that the mass-weighted, vertically integrated radiative cooling of the atmosphere is equal to the turbulent moist static energy flux at the sea surface.

Quantitative assessments of radiative-convective equilibrium states can be made using one-dimensional column models that solve radiative transfer equations and contain representations of moist convective transports. The equilibrium water vapor profiles obtained in such calculations are very sensitive to assumptions about the way cloudy air mixes with its environment, and about the detailed microphysical processes governing the production, fall and re-evaporation of precipitation. (See Rennó et al. [12] for a detailed treatment of this problem.) Given the limited understanding of these processes, one strategy is to optimize the parameters governing such processes in the representation of convection in such a way that the prediction of relative humidity is in best accord with observations. (See Emanuel and Zivkovic-Rothman [6] for a detailed treatment of this approach.) An example of the profile of relative humidity produced by such a model, run into a state of radiative-convective equilibrium, is shown in Figure 1.10. There is a pronounced minimum in the middle to upper troposphere, and the tropopause is close to saturation with respect to ice. (Near the tropopause, the detrainment of water substance from the tops of deep clouds cannot be balanced by drying by subsidence, which vanishes there.) The vertical profile of moist static energy in this equilibrium state is illustrated in Figure 1.11. Of considerable interest and importance is the pronounced minimum in  $h$  in the lower to middle troposphere. This is also observed throughout the actual Tropics. As air sinks between clouds, it loses energy, owing to radiative cooling, but in the lower troposphere this loss is more than compensated by the convergence of the upward flux of  $h$  by clouds. The radiative and moist static energy fluxes are shown in Figure 1.12.

In recent years, it has become possible to explicitly simulate radiative-convective equilibrium using three-dimensional, cloud-resolving, nonhydrostatic numerical models that include representations of cloud micro-

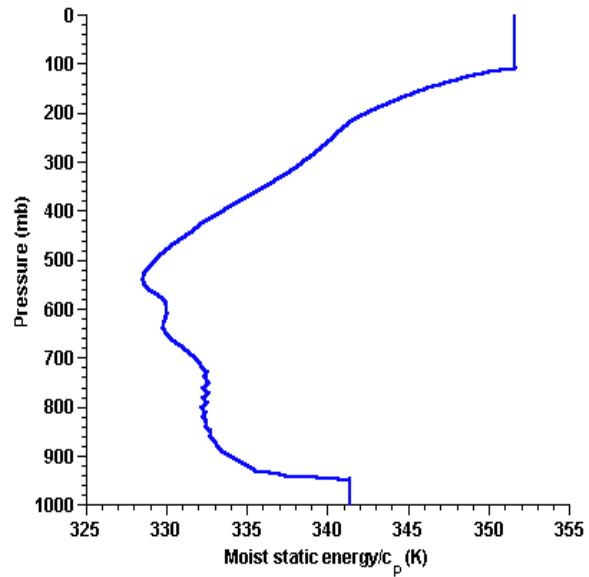


Figure 1.11: Same as in figure (1.10), but showing the equilibrium profile of moist static energy.

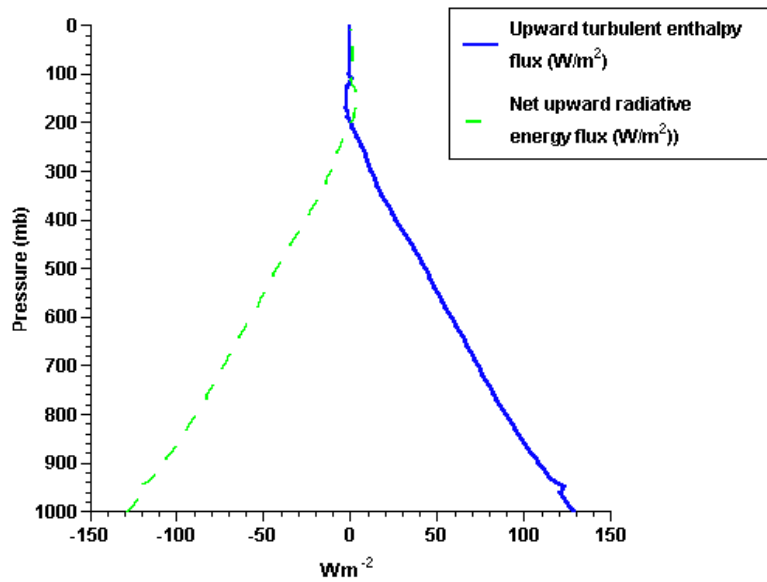


Figure 1.12: Same as in figure (1.10), but showing the radiative and turbulent enthalpy fluxes.



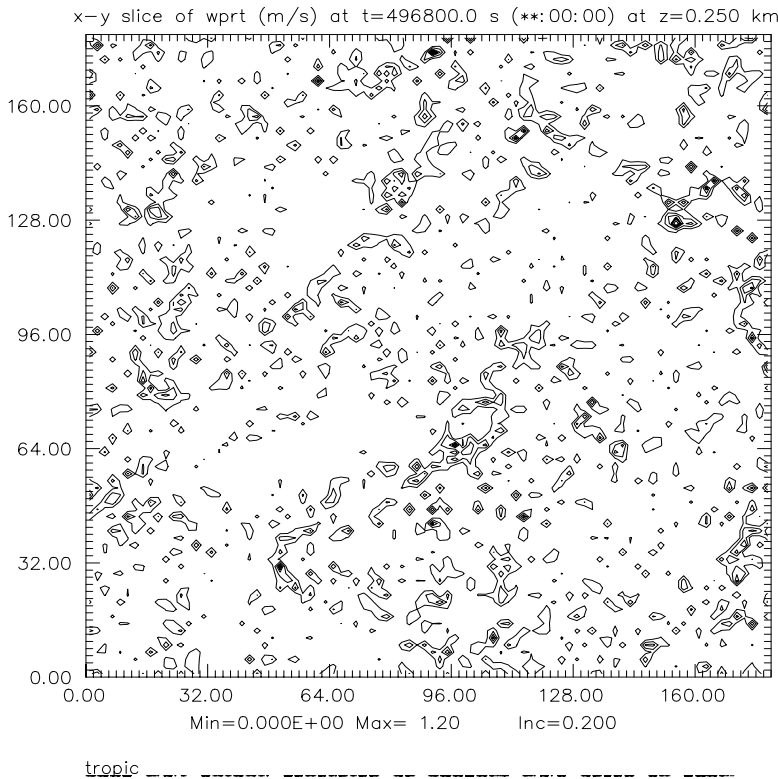


Figure 1.13: **Distribution of vertical velocity at 250 m altitude in a state of statistical radiative-convective equilibrium in a  $180 \times 180 \text{ km}^2$ , doubly periodic domain forced by specified radiative cooling in the troposphere. From Robe and Emanuel [13].**

physical processes and subgrid-scale transports. What is generally done is to specify a fixed ocean temperature and to either specify or calculate the radiative cooling of the atmosphere. The model is run in a square domain with doubly periodic lateral boundaries, and the domain is large enough to contain many clouds at the same time. The model is run into a state of statistical equilibrium, in which the domain-averaged properties have achieved some statistical stability. The actual dynamics are chaotic, of course.

Figure 1.13 shows a snapshot of the distribution of vertical velocity near the top of the subcloud layer in one such run, described in detail by Robe and Emanuel [13]. Relatively strong updrafts mark the bases of individual clouds. The vertical distribution of temperature and moisture in this simulation closely resembles those of the single-column model described above.

Figure 1.14 summarizes the energy balance of the global atmosphere. Of 100 units of incoming solar radiation, about 30% is reflected back to space by the surface, by clouds, and by the atmosphere itself. A small amount of solar radiation is directly absorbed in the atmosphere, mostly by water vapor and by clouds. The back radiation of the atmosphere to the earth is so large - larger than the incoming solar radiation reaching the surface - that there must be large convective energy transport away from the surface. It is conventional to divide this turbulent energy transport into two parts: sensible and latent flux. The latter is proportional to rate of evaporation of water from the surface into the overlying air. Note that most

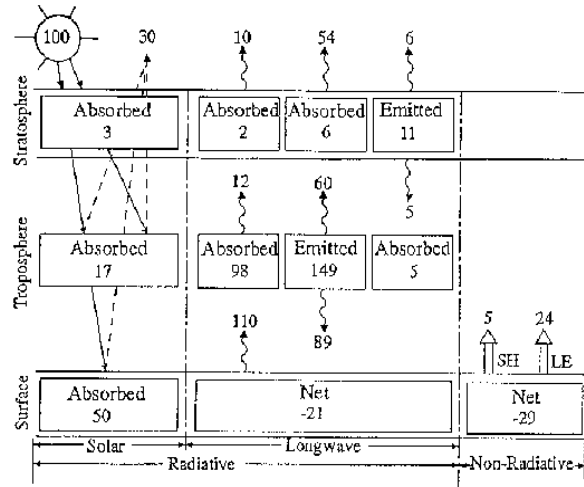


Figure 1.14: Radiative and turbulent energy flux diagram for the earth and atmosphere. Incoming solar radiation set arbitrarily to 100 units.

of the flux is in the form of latent heat flux. In fact, in the Tropics, the latent heat flux is very much larger than either the sensible flux or the net longwave radiative flux from the surface. So, to a good approximation, absorption of solar radiation by the tropical oceans is balanced by cooling by evaporation.

To maintain the large turbulent energy flux away from the surface, the tropical atmosphere and ocean must exist in a state of considerable thermodynamic disequilibrium. To see this, it is helpful to examine a conventional formula for estimating the energy flux,  $E$ , from the ocean to the atmosphere:

$$E \simeq C_q \rho |\mathbf{V}| (k_0^* - k), \quad (1.29)$$

where  $C_k$  is a dimensionless exchange coefficient,  $\rho$  is the air density,  $|\mathbf{V}|$  is the magnitude of the wind speed near the surface,  $k$  is the specific enthalpy of the air, and  $k_0^*$  is the saturation specific enthalpy of air at sea surface temperature and pressure. It is conventional to evaluate all the quantities in (1.29), except for  $k_0^*$ , at an altitude of 10 meters above the surface. ( $C_k$  is calibrated to this altitude.)

One can see from (1.29) that to maintain large evaporation rates, one must have a large degree of thermodynamic disequilibrium, as given by the term  $(k_0^* - k)$ , and this degree of disequilibrium is inversely proportional to the average wind speed, for a given evaporation rate. Tropical cyclones, and perhaps other tropical phenomena, use this disequilibrium to fuel their power consumption, as we illustrate in the last chapter.

## 2 The Zonally Averaged Circulation

### 2.1 The observed climatology

The general flow of air in the Tropics is dominated by planetary and regional scale circulations that vary on seasonal to interannual time scales; these space and time scales are considerably larger than those of mid- and high-latitude weather. Suitably time-averaged precipitation also shows slow variation in space and time, but rainfall is dominated by convection, which has intrinsically short space and time scales (typically  $10-100\text{ km}$  and a few hours). Maps of air seasonal mean air flow near the surface and precipitation are shown in Figure 2.1 and Figure 2.2. Note that in many ranges of longitude, the distributions are nearly zonal. The constancy of wind circulation systems in the Tropics led early theorists (e.g. Halley and Hadley) to suggest that the general circulation is nearly zonally symmetric. While that characterization fails dramatically in middle and high latitudes, it is not so far off the mark in the Tropics. It proves useful to consider the circulation of the tropical atmosphere to consist of a slowly varying, zonally-symmetric component on which is superimposed certain slow, zonally varying circulations as well as higher frequency motions.

Figure 2.3 shows the zonally averaged mass streamfunction in northern hemisphere summer and in northern hemisphere winter. The strongest overturning circulation is in the tropics, with upward motion extending from about  $10^\circ$  on the winter side of the equator to about  $20^\circ$  on the summer side. Likewise, there is strong descent in the winter hemisphere subtropics. Note also that there are much weaker and narrower thermally direct overturning cells in the summer hemisphere. These tropical overturning cells are known as the Hadley circulation. Much of the mass transport in the Tropics is accomplished by these zonally symmetric overturning motions, in contrast to higher latitudes, where much of the transport is associated with transient, zonally varying wind systems. The corresponding zonally averaged meridional and vertical velocities are shown in Figure 2.4. Note that the meridional velocity associated with the Hadley overturning is strongly concentrated near the surface and near the tropopause. There is hardly any mean meridional motion outside the Tropics.

The distributions of zonally averaged zonal velocity, temperature and specific humidity are shown respectively in Figure 2.5, Figure 2.6 and Figure 2.7, for both extreme seasons. Zonal jets are concentrated near the tropopause around  $30^\circ-40^\circ$  latitude; stronger and closer to the equator in the winter hemisphere. The deep Tropics are characterized by weak easterlies throughout the troposphere. The horizontal temperature gradient is extremely weak in the tropics, and almost all the water vapor in the atmosphere resides in the tropical lower troposphere.

### 2.2 The zonally symmetric radiative-convective equilibrium

To understand why there is any overturning circulation at all, it is helpful to first attempt to construct an exact solution of the governing equations containing no such circulation. We will see that, under certain circumstances, such a solution cannot be realized; we will then show that this ill-posedness of the radiative-convective equilibrium state implies the existence of overturning circulations.

Let us imagine, then, a zonally symmetric planet subject to incident solar radiation that is symmetric about the equator (say, the incident radiation at equinox). At each latitude, we calculate the one-dimensional radiative-convective equilibrium solution. Of course, the temperature at each pressure level may be expected to decrease poleward, implying through the hydrostatic equation that at each level, except possibly for one, there must exist meridional pressure gradients. We will suppose that such gradients are in gradient-wind balance with a zonal wind.

For this equilibrium to be steady, there must be no dissipation associated with the zonal wind. This

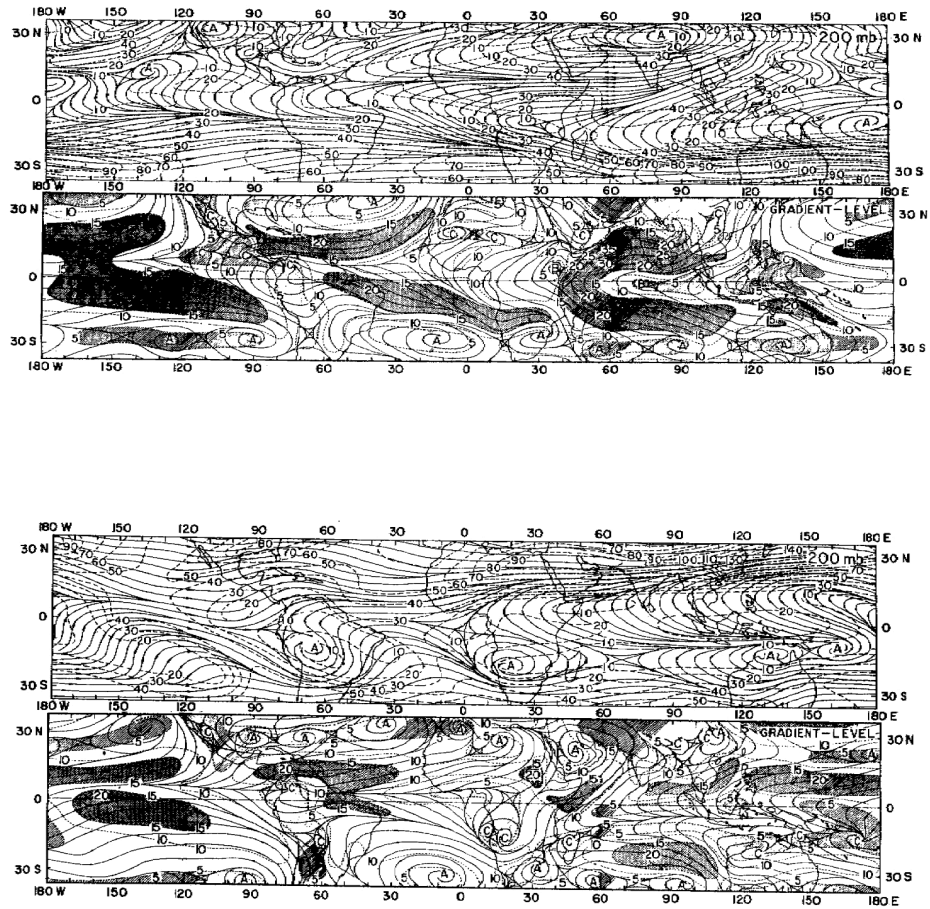


Figure 2.1: Circulation over the global tropics in July (top figure) and January (bottom figure). Wind streamlines, and isotachs in knots at 200 mb (top panels) and near 850 mb (bottom panels).

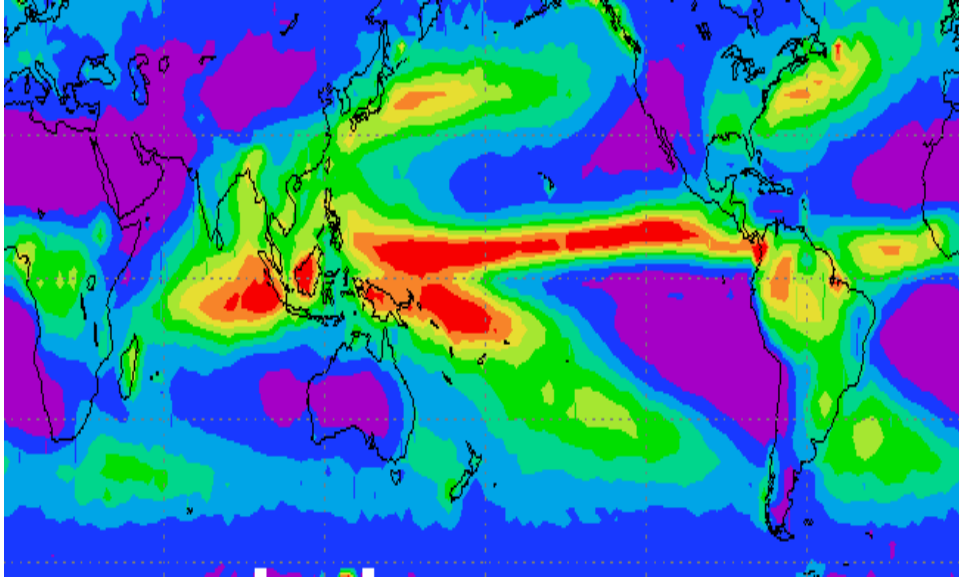


Figure 2.2: **Global distribution of annual-average precipitation.**

may be a good approximation away from the surface, given the stable stratification of the atmosphere, but cannot work right next to the surface. To get around this, we suppose that the surface wind (and thus the meridional pressure gradient) vanishes in our equilibrium solution. We can arrange this to be the case thanks to the integration constant that arises in integrating the hydrostatic equation upward. (In other words, we choose the surface to be the level of vanishing horizontal pressure gradient.)

So at each latitude, we have the density temperature profile from our radiative-convective equilibrium solution, and we integrate upward the hydrostatic equation, in the form

$$\frac{\partial \phi}{\partial p} = -\alpha = -\frac{R_d T_p}{p}, \quad (2.1)$$

setting as a boundary condition  $\phi = 0$  at  $p = p_0$ , where  $p_0$  is the fixed surface pressure. We will then have geopotential as a function of both pressure and latitude, and we can solve the gradient wind equation to find the zonal wind, also as a function of latitude and pressure. Alternatively, we can differentiate (2.1) in latitude and use gradient wind balance to derive a thermal wind relation, which can then be integrated upward, starting from the boundary condition that  $u = 0$  at  $p = p_0$ .

The gradient wind equation, in spherical coordinates, may be written

$$\frac{\partial \phi}{\partial \theta} = -2\Omega a \sin \theta u - \tan \theta u^2, \quad (2.2)$$

where  $\theta$  is latitude,  $a$  is the earth's radius,  $\Omega$  is the angular velocity of the earth's rotation, and  $u$  is the zonal velocity. It is more convenient to express (2.2) in terms of angular momentum per unit mass,  $M$ , rather than zonal velocity, since for zonally symmetric, inviscid motions,  $M$  is conserved. The angular momentum per unit mass is (under the approximation that the atmosphere is a thin shell)

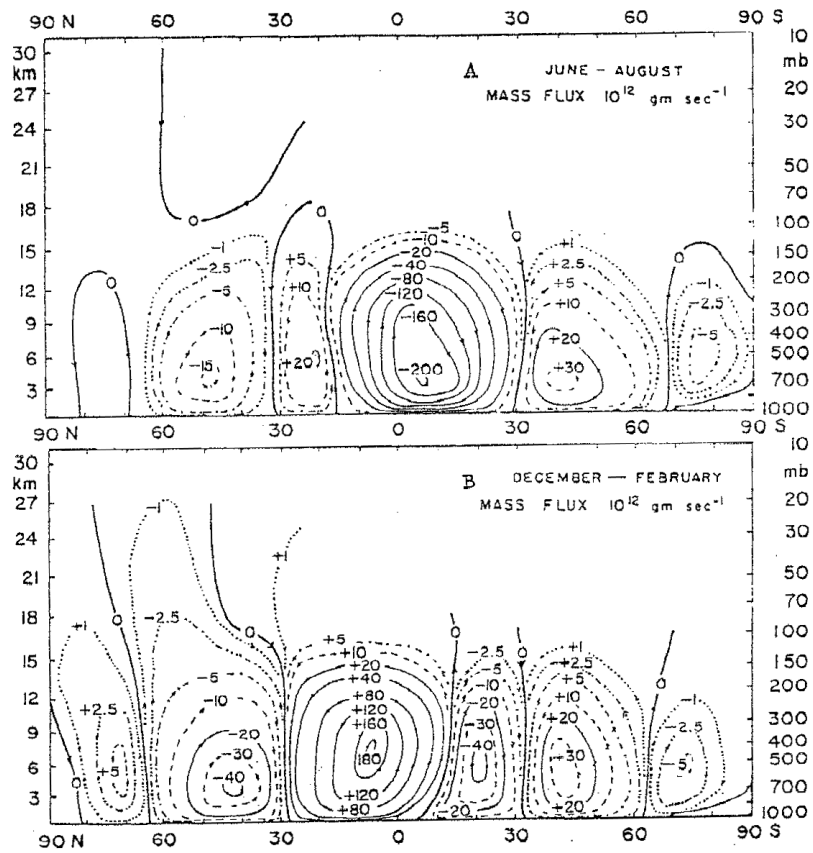


Figure 2.3: Climatological zonal-mean mass streamfunction. From Newell et al., 1972 [9].

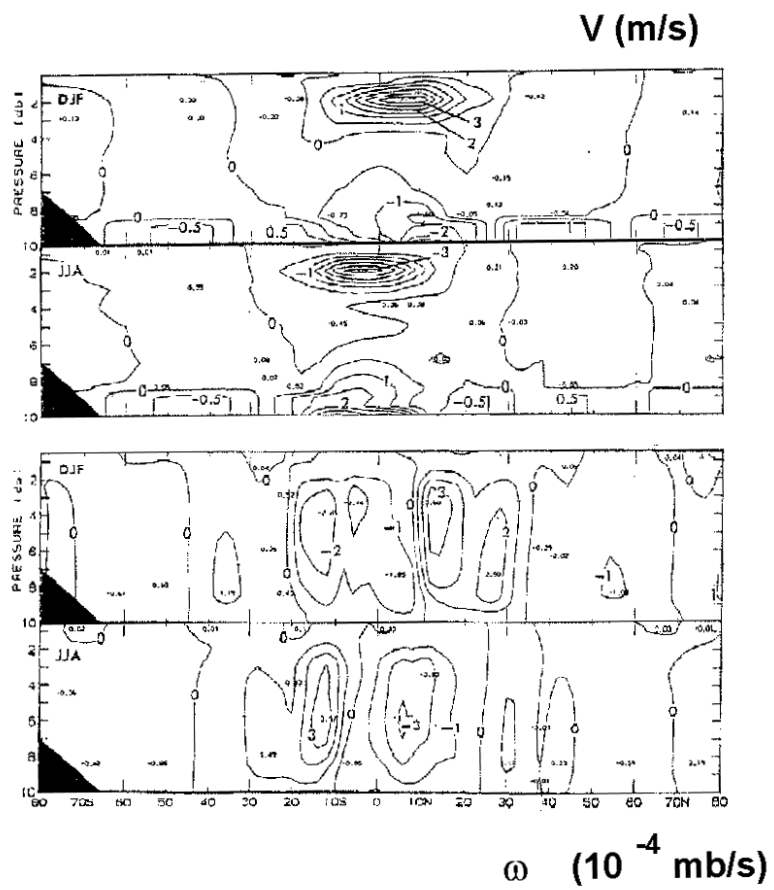


Figure 2.4: Zonal mean northward component of velocity, and pressure velocity ( $\omega$ ) in a ten-year climatology. From Oort, 1983 [10].

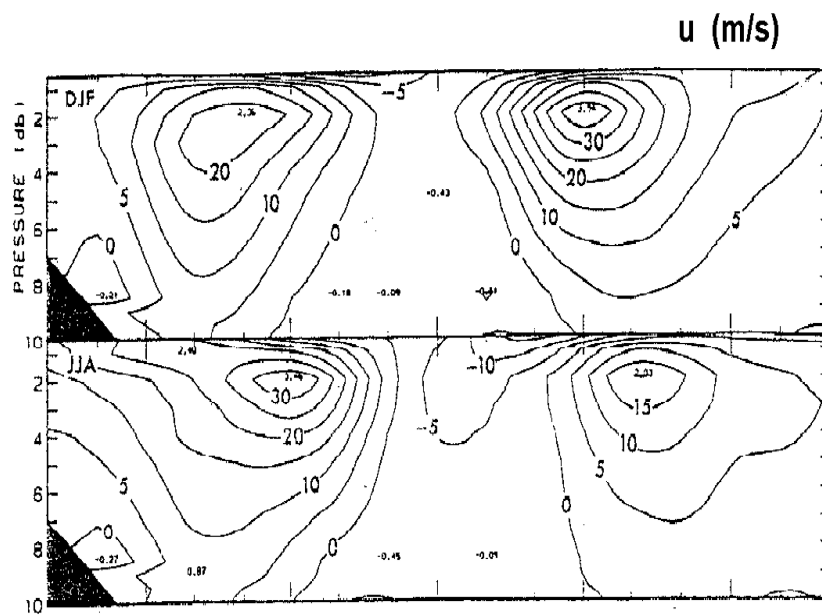


Figure 2.5: Zonal mean zonal winds from a ten-year climatology. From Oort, 1983 [10].



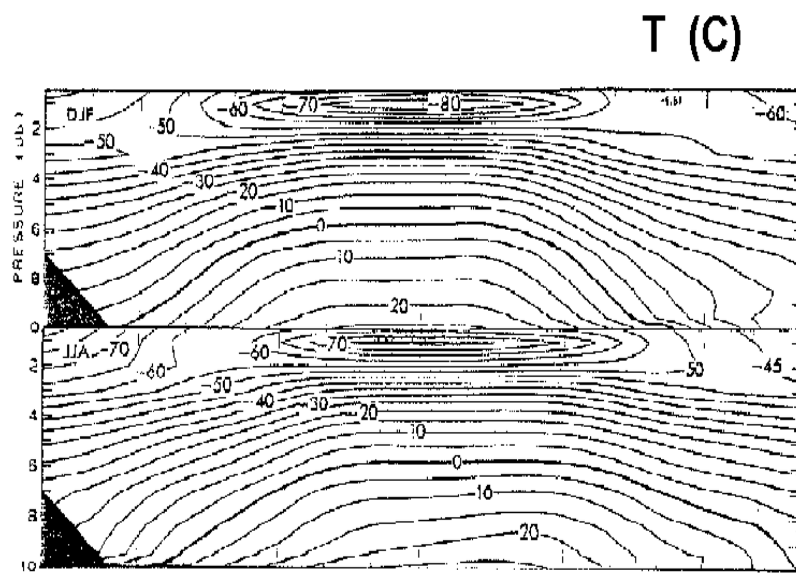


Figure 2.6: Zonal mean temperature from a ten-year climatology. From Oort, 1983 [10].

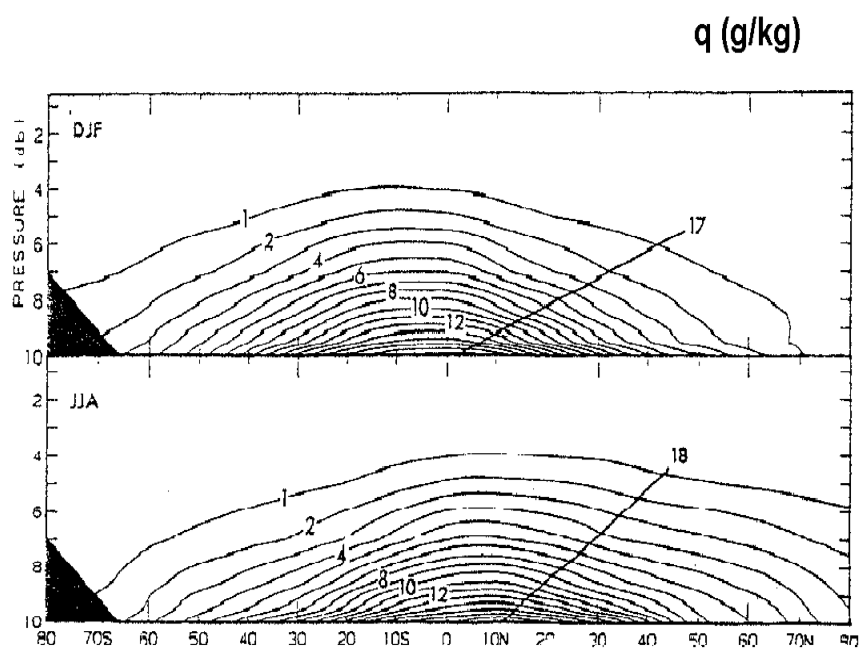


Figure 2.7: Zonal mean specific humidity from a ten-year climatology. From Oort, 1983 [10].

$$M = a \cos \theta (\Omega a \cos \theta + u). \quad (2.3)$$

In terms of  $M$ , (2.2) may be written

$$\frac{\partial \phi}{\partial \theta} = -\sin \theta \left[ \frac{M^2 - \Omega^2 a^4 \cos^4 \theta}{a^2 \cos^3 \theta} \right]. \quad (2.4)$$

Cross-differentiating (2.1) and (2.4) then gives the thermal wind equation:

$$\frac{1}{a^2} \frac{\tan \theta}{\cos^2 \theta} \frac{\partial M^2}{\partial p} = \left( \frac{\partial \alpha}{\partial \theta} \right)_p. \quad (2.5)$$

Since  $\alpha$  is known as a function on latitude and height from the radiative-convective equilibrium model, (2.5) may be integrated upward to find  $M$  (and therefore  $u$ ) as a function of height, starting from  $u = 0$  at the surface.

A considerable simplification results in this development from the fact that the radiative-convective equilibrium state is very nearly neutral to moist convection. We showed in the previous chapter that moist convective neutrality is characterized by a state in which samples lifted reversibly and adiabatically from close to the surface have about the same density temperature as their environment. Here, for the sake of simplicity, we will neglect the effect of variable water content on density, and approximate this state as one in which the actual temperature of a lifted sample is equal to that of its environment.

Suppose we define a state variable called the *saturation entropy*,  $s^*$ , as follows:

$$s^* \equiv (c_{pd}(1 - q_t) + c_1 q_t) \ln(T) - R_d \ln(p_d) + \frac{L_v q^*}{T}, \quad (2.6)$$

where  $q^*$  is the saturation specific humidity, which is a function of pressure and temperature.

Note that if the air is saturated, the saturation entropy given by (2.6) is equal to its actual entropy, as given by (1.21). We also note that, neglecting for the moment the differing values of  $q_t$ , air inside a cloud will have the same temperature as air outside the cloud at the same pressure if their saturation entropies are equal. But the saturation entropy of air inside the cloud is equal to its actual entropy, since cloud air is, by definition, saturated. Moreover, the air lifted inside the cloud is supposed to conserve its entropy, so that the latter is constant with height. It follows from these arguments that *in a convectively neutral atmosphere, the saturation entropy,  $s^*$ , is approximately constant with altitude in the cloud-bearing layer*. The approximation of saturation entropy constant with height allows us to reduce the description of the latitudinally varying equilibrium state to a one-dimensional problem, as demonstrated presently.

Once again neglecting the dependence of density on variable water content, we may express  $\alpha$  as a function of any other two state variables, say, pressure and saturation entropy:

$$\alpha = \alpha(s^*, p). \quad (2.7)$$

We may therefore express variations of  $\alpha$  at constant pressure by

$$(\delta \alpha)_p = \left( \frac{\partial \alpha}{\partial s^*} \right)_p \delta s^*. \quad (2.8)$$

It is convenient to express the right hand side of (2.8) by using one of Maxwell's relations, derived from the first law of thermodynamics (e.g. see Emanuel, 1986 [3]):

$$\left(\frac{\partial\alpha}{\partial s^*}\right)_p = \left(\frac{\partial T}{\partial p}\right)_{s^*}. \quad (2.9)$$

Thus (2.8) may be expressed

$$(\delta\alpha)_p = \left(\frac{\partial T}{\partial p}\right)_{s^*} \delta s^*. \quad (2.10)$$

Using (2.10), we may thus write (2.5) as

$$\frac{1}{a^2} \frac{\tan\theta}{\cos^2\theta} \frac{\partial M^2}{\partial p} = \left(\frac{\partial T}{\partial p}\right)_{s^*} \frac{\partial s^*}{\partial\theta} \quad (2.11)$$

The beauty of expressing the left side of (2.11) in terms of  $s^*$  is that, in a convectively neutral atmosphere,  $s^*$  is nearly independent of pressure, so that (2.11) may be integrated exactly in pressure. Moreover, convective neutrality demands that  $s^*$  at altitude is equal to the actual entropy of the boundary layer, which we will call  $s_b$ . Using this and applying the boundary condition  $u = 0$  at  $p = p_0$  gives, when integrating (2.11),

$$M^2 = a^2 \cos^2\theta \left[ \Omega^2 a^2 \cos^2\theta - ctn\theta (T_b - T) \frac{\partial s_b}{\partial\theta} \right], \quad (2.12)$$

where  $T_b(\theta)$  is the absolute temperature in the boundary layer. This gives the distribution of zonal velocity in terms of the latitudinal distribution of the boundary layer entropy,  $s_b$ , while its vertical variation is given by the difference between the absolute temperature at the latitude in question and the boundary layer temperature at the same latitude.

To the extent that the only friction is at the surface, (2.12) represents an exact equilibrium solution of all the governing equations. Since each column is in radiative-convective equilibrium and the horizontal pressure gradient acceleration is balanced at each point by Coriolis accelerations associated with the zonal wind, we have no net tendency of temperature or wind, and every quantity is in equilibrium. But there is no meridional or vertical flow associated with this solution, so why do we need a Hadley circulation?

### 2.3 Viability of the equilibrium state

In some cases, the equilibrium solution given by (2.12) is not viable, for reasons that can be summed up by the expression, often heard in Maine, that “you can’t get there from here”. The history of the extant ideas about this include Schneider and Lindzen (1977)[14], Schneider (1977)[15], Held and Hou (1980)[7], Lindzen and Hou (1988)[8], and Plumb and Hou (1992)[11]. Here we closely follow Emanuel (1995)[5].

Suppose we try to spin up to the equilibrium solution starting from a state of rest. Here the angular momentum is everywhere equal to the planetary angular momentum, which reaches its maximum value on the equator. In the process of spinning up, angular momentum is conserved, so it follows that *nowhere can the angular momentum reach a value that exceeds that of air at rest on the equator*. We can see immediately from (2.12) that

$$(T_0 - T) \frac{\partial s_b}{\partial\theta} \geq - \frac{\Omega^2 a^2 \tan\theta (1 - \cos^4\theta)}{\cos^2\theta} \quad (2.13)$$

must be obeyed. Thus, if the radiative-convective equilibrium distribution of entropy has too strong an equatorward gradient, (2.12) cannot be realized. Since the right-hand side of (2.13) vanishes at the equator,

ANY equilibrium entropy gradient across the equator invalidates (2.12). Note that the largest magnitude of the left side of (2.13) will be realized at the tropopause, where  $T_0 - T$  has its maximum value, so the breakdown occurs first at the tropopause. But we can place an even more stringent requirement on the viability of (2.12): *there can be no extremum of angular momentum away from the surface*. If there were, even the slightest bit of diffusion would destroy the maximum, which could not be replaced by advection owing to the conservation of  $M$ . Thus, among other things, *the meridional gradient of angular momentum must always be toward the equator*. This is equivalent to stating that *the vertical component of absolute vorticity must always have the same sign as the Coriolis parameter, or be zero*. From (2.12) we have that

$$4\Omega^2 a^2 \cos^3 \theta + \frac{1}{\sin \theta} \frac{\partial}{\partial \theta} \left[ \cos^2 \theta \operatorname{ctn} \theta (T_s - T_t) \frac{\partial s_b}{\partial \theta} \right] > 0, \quad (2.14)$$

where  $T_t(\theta)$  is the temperature at the tropopause.

By making the substitution

$$y \equiv \sec^2 \theta, \quad (2.15)$$

we can express (2.16) more simply as

$$1 + y^3 \frac{\partial}{\partial y} \left[ \frac{T_s - T_t}{\Omega^2 a^2} \frac{\partial s_b}{\partial y} \right] > 0. \quad (2.16)$$

Thus if the negative curvature of the equilibrium entropy distribution in latitude exceeds a latitude-dependent threshold, the equilibrium solution cannot be maintained.

We shall next show that such a breakdown implies the existence of a thermally direct overturning circulation.

## 2.4 Construction of a Hadley equilibrium state

We shall suppose that when the radiative-convective equilibrium solution is not viable, an overturning circulation exists in its place. Suppose that most of the frictional dissipation associated with such a circulation occurs in the boundary layer. In that case, angular momentum will be conserved above the boundary layer. Since the streamlines of any such circulation must be parallel to the tropopause, just below the tropopause, and since angular momentum is conserved there, it follows that angular momentum surfaces must be flat in that region; i.e., there is no meridional gradient of angular momentum.

Suppose that, as a first attempt to construct a solution, we first relax our previous requirement that the zonal flow vanishes at the surface, and instead integrate (2.11) down from the tropopause, insisting that  $M$  equals its resting value at the equator there. (That is, we assume that the ascent is centered at the equator and that the air carries upward the angular momentum of air at rest there.) The result is

$$M^2 = \Omega^2 a^4 + a^2 \cos^2 \theta \operatorname{ctn} \theta \frac{\partial s^*}{\partial \theta} (T - T_t). \quad (2.17)$$

Inverting this to find  $u$  gives

$$u = \sqrt{\Omega^2 a^2 \sec^2 \theta + \operatorname{ctn} \theta \frac{\partial s^*}{\partial \theta} (T - T_t)} - \Omega a \cos \theta. \quad (2.18)$$

Since the saturation entropy decreases poleward,  $u < 0$  close to the equator and reaches its maximum magnitude at the surface. Sufficiently far from the equator, the surface wind is westerly. But because there

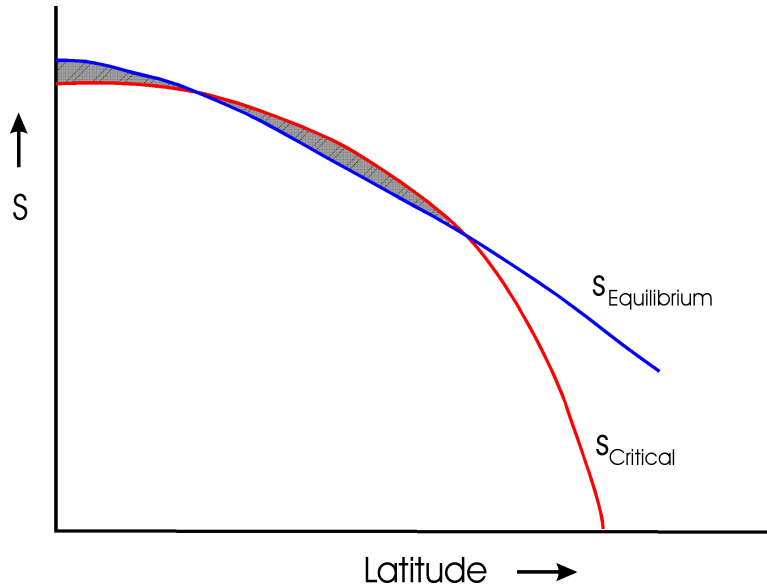


Figure 2.8: Critical and radiative-convective equilibrium entropy curves, showing equal-area assumption.

is now a surface wind, there must be frictional dissipation, and surface friction acting on surface easterlies will cause an Ekman flow toward the equator. This in turn implies ascent there, as we postulated originally.

There are several problems with this solution, however. First, since the surface wind is everywhere easterly, the earth is constantly losing angular momentum to the atmosphere; this cannot be an equilibrium solution. Second, although we can imagine the streamlines following angular momentum surfaces as they emerge from the boundary layer near the equator, and also as they bend over and flow poleward near the tropopause, they do have to close somewhere. But where they bend over, the angular momentum surfaces must do so also, and this violates the principle that angular momentum may not have an extremum away from the surface. The only way around this is to require dissipation somewhere in the flow aloft, so that the streamlines may cross angular momentum surfaces in the steady state. *The zonally symmetric solution, also symmetric about the equator, requires dissipation above the boundary layer.* In dissipating kinetic energy, the associated turbulence must also serve to transfer angular momentum poleward, inducing surface westerlies at higher latitudes.

Held and Hou (1980)[7] developed a cleaner solution to the problem of what happens when the critical condition is violated. They supposed that the resulting thermally direct circulation acts to restore the actual temperature (entropy) distribution to very close to its critical distribution. (The scaling behind this argument was explored further by Emanuel (1995)[5].) They recognized that, in general, the critical entropy distribution curve crosses the actual entropy distribution curve in two places, as illustrated in Figure 2.8.

They reasoned that the solution would resemble the critical curve in the region where the equilibrium entropy distribution is supercritical, while the equilibrium solution would obtain in higher latitudes, where it is subcritical. The boundary between the regions is determined by two conditions. The first is simply that the entropy must be continuous across the boundary separating the two regions. The second assumes that for small departures from radiative-convective equilibrium, the rate of radiative heating/cooling is linearly proportional to the difference between actual and equilibrium entropies. Since there can be no net heating,

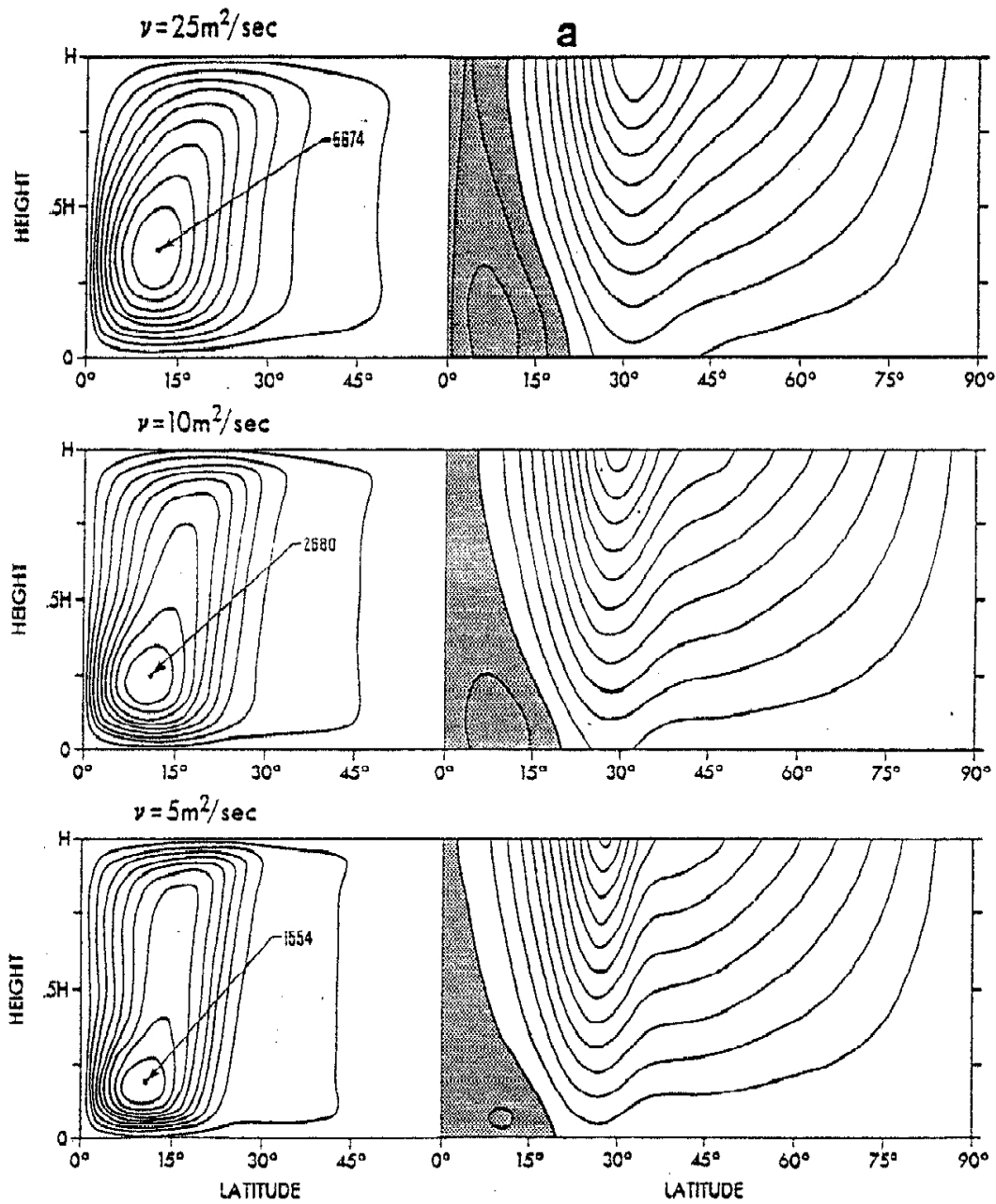


Figure 2.9: Calculated distributions of mass streamfunction (left) and zonal wind (right), from Held and Hou (1980)[7], as a function of the magnitude of the eddy diffusivity used in the model, shown in upper left of each panel. The maximum value of the streamfunction is shown, and the shading in the zonal wind figures denotes easterlies.

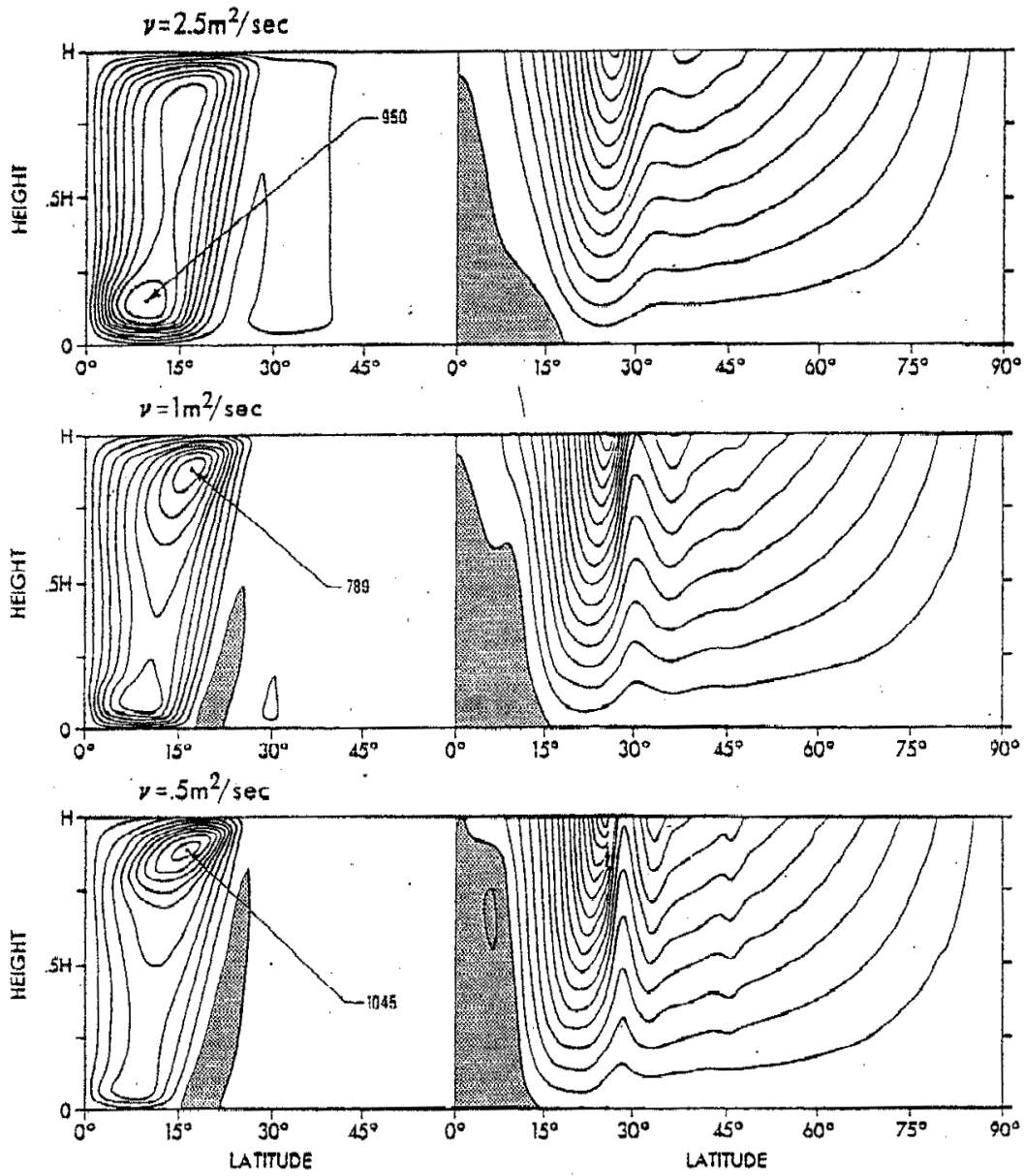


Figure 2.10: Continuation of Figure 2.9.



integrated in latitude, it follows that

$$\int_0^{90} (s_{critical} - s_{equilibrium}) \cos(\theta) d\theta = 0. \quad (2.19)$$

Thus the shaded areas shown in Figure 2.8 must sum to zero if the x axis is linear in  $\sin(\theta)$ . An estimate of the magnitude of the overturning circulation can be readily made by evaluating the local energy balance in equilibrium:

$$c_p w \frac{\partial \Theta}{\partial z} = \frac{\Theta}{T} Q_{net}, \quad (2.20)$$

where  $w$  is the vertical velocity,  $\Theta$  is the potential temperature, and  $Q_{net}$  is the net heating of the column. In (2.20) the horizontal temperature advection has been neglected. Since the vertical distribution of  $\Theta$  will, in practice, closely resemble its distribution along a moist adiabat, (2.20) can be readily evaluated to make an estimate of the vertical velocity at each point in the Hadley regime.

Held and Hou (1980)[7] also ran a two-dimensional (zonally symmetric) numerical model forced by Newtonian relaxation of temperature back to a profile that decreases with latitude as  $\sin^2(\theta)$ . The distributions of mass streamfunction and zonal velocity in the steady state are shown as a function of the magnitude of the eddy diffusivity used in the model in Figure 2.9 and Figure 2.10.

There is clearly a strong dependence of the magnitude of the overturning rate on the value of the eddy diffusivity used in the model, with decreasing diffusivity leading to decreased overturning. It is not clear whether the magnitude of the mass streamfunction is converging to a finite value at very low diffusivity; when the diffusivity is very small there may be numerical problems with the simulation. On the other hand, the distribution of zonal velocity does seem to converge to the inviscid solution, as demonstrated by Figure 2.11.

## 2.5 The slantwise neutral solution

Any solution in which the angular momentum varies with height but which is neutral to gravitational, moist convection will be nonetheless unstable to a form of moist convection driven by a combination of gravitational and Coriolis accelerations (Emanuel, 1983a and b [1],[2]). This has been called *slantwise convection*. It is possible to construct solutions that are in radiative-*slantwise* convective equilibrium and which satisfy thermal wind balance. To do this, we start from the thermal wind equation, (2.11). In the slantwise neutral state, the saturation moist entropy,  $s^*$ , is constant along angular momentum surfaces, rather than in the vertical (see [1] and [2]). This means that  $s^* = s^*(M)$ , so that (2.11) can be written

$$\frac{1}{a^2} \frac{\tan \theta}{\cos^2 \theta} \frac{\partial M^2}{\partial p} = \left( \frac{\partial T}{\partial p} \right)_{s^*} \frac{ds^*}{dM^2} \frac{\partial M^2}{\partial \theta}. \quad (2.21)$$

Now divide each side of (2.21) by  $\frac{\partial M^2}{\partial p}$ , and make use of the fact that

$$\frac{\partial M^2 / \partial \theta}{\partial M^2 / \partial p} = - \left( \frac{\partial p}{\partial \theta} \right)_M.$$

Then (2.21) becomes

$$\frac{1}{a^2} \frac{\tan \theta}{\cos^2 \theta} \left( \frac{\partial \theta}{\partial p} \right)_M = - \left( \frac{\partial T}{\partial p} \right)_{s^*} \frac{ds^*}{dM^2}. \quad (2.22)$$

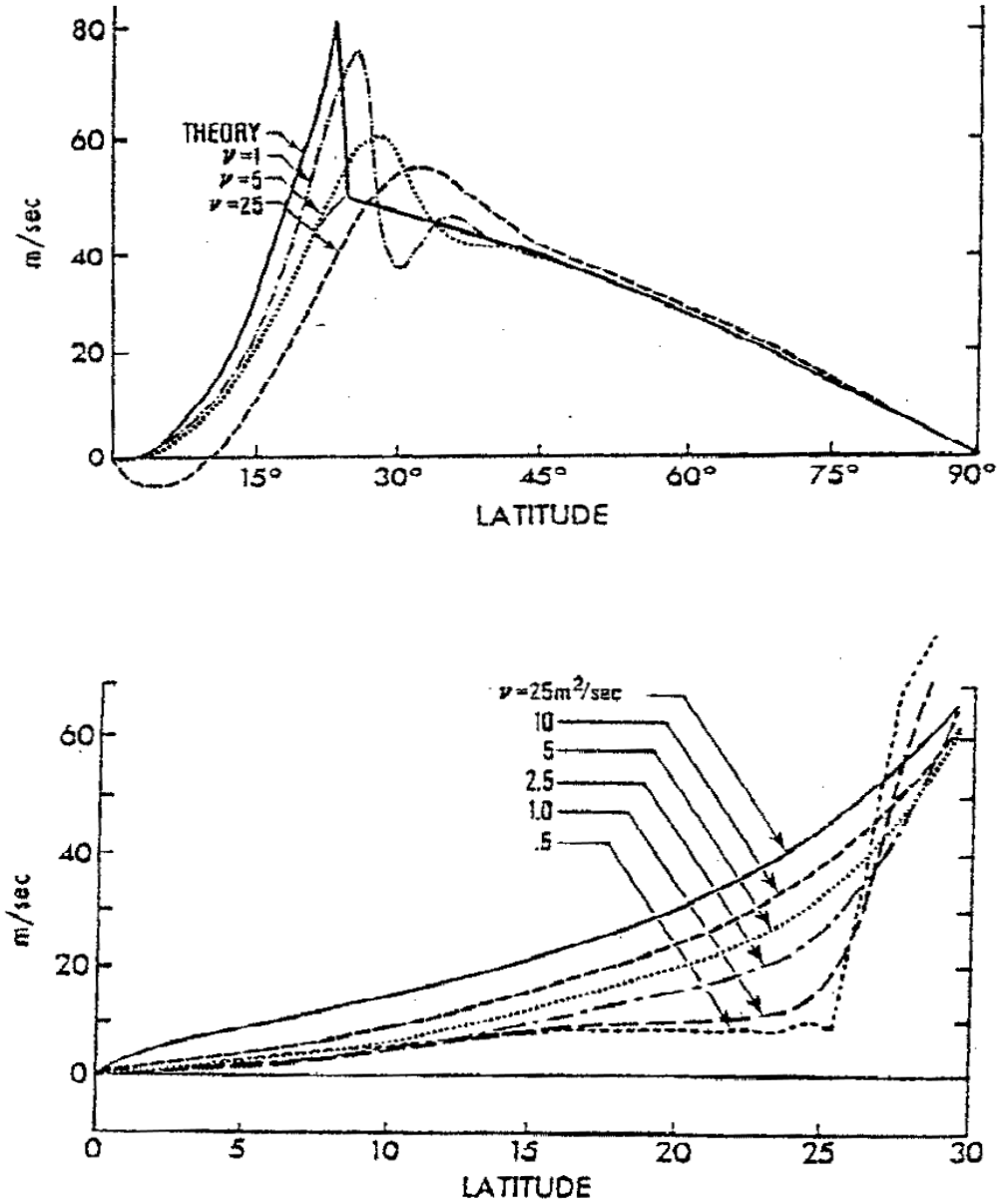


Figure 2.11: Distributions of zonal wind (top) and the quantity  $\Omega a \sin^2(\theta) - u \cos(\theta)$ , proportional to the absolute angular momentum, (bottom) in the numerical and theoretical solutions of Held and Hou (1980)[7].

This is an equation for the slope of angular momentum (and  $s^*$ ) surfaces. Since  $s^* = s^*(M)$ , it follows that  $\frac{ds^*}{dM^2}$  is also only a function of  $M$ , so that (2.22) can be directly integrated upward *along  $M$  surfaces*. The result of doing this is an equation for the latitude of particular  $M$  (or  $s^*$ ) surfaces:

$$\tan^2\theta = \tan^2\theta_b + 2a^2 \frac{ds^*}{dM^2} (T_b - T), \quad (2.23)$$

where  $\theta_b$  and  $T_b$  are the latitude and temperature of the  $M$  surface in question at the top of the boundary layer. Assuming that there is no zonal flow at the surface, we can use

$$\frac{ds^*}{dM^2} = \frac{(\partial s_b / \partial \theta)}{(\partial M^2 / \partial \theta)_b} = -\frac{1}{4\Omega^2 a^4 \cos^3\theta_b \sin\theta_b} \frac{\partial s_b}{\partial \theta}, \quad (2.24)$$

so that (2.23) becomes

$$\tan^2\theta = \tan^2\theta_b - \frac{1}{2\Omega^2 a^2 \cos^3\theta_b \sin\theta_b} \frac{\partial s_b}{\partial \theta} (T_b - T). \quad (2.25)$$

It is clear from (2.25) that the  $M$  surface that originates at the surface on the equator will end up off the equator if the equilibrium entropy decreases sufficiently fast away from the equator, just as in the classical (Held-Hou) solution. In the particular case that the equilibrium entropy varies as  $\sin^2\theta$ , the  $M$  surface that begins at the surface at the equator winds up a finite distance off the equator as one moves upward in the troposphere. Within that particular  $M$  surface, one might expect that both the saturation entropy ( $s^*$ ) and the angular momentum ( $M$ ) are homogenized.

As an example, suppose the radiative-slantwise convective equilibrium solution for entropy is

$$s_b = s_e - \Delta s \sin^2\theta, \quad (2.26)$$

where  $s_e$  is the equatorial value of equilibrium entropy and  $\Delta s$  is the pole-to-equator equilibrium entropy difference. Substituting into (2.25) and applying a little trigonometry gives

$$\cos^2\theta = \frac{\cos^2\theta_b}{\left[1 + \frac{\Delta s (T_b - T)}{\Omega^2 a^2}\right]}. \quad (2.27)$$

In particular, the latitude,  $\theta_c$ , that bounds the region of homogenized  $M$  and  $s^*$  near the equator is given by

$$\cos^2\theta_c = \frac{1}{\left[1 + \frac{\Delta s (T_b - T)}{\Omega^2 a^2}\right]}. \quad (2.28)$$

Inside this bounding surface,  $s^* = s_e$  and  $M$  is constant and equal to its rest value on the equator, giving

$$u = \Omega a \tan\theta \sin\theta, \quad (2.29)$$

whereas outside the bounding surface, we have on each  $(M, s^*)$  surface

$$s^* = s_b, \quad (2.30)$$

and

$$\begin{aligned}
u &= \frac{M_b}{a \cos \theta} - \Omega a \cos \theta \\
&= \Omega a \left[ \frac{\cos^2 \theta_b}{\cos \theta} - \cos \theta \right].
\end{aligned}$$

Using (2.27) for  $\theta_b$  then gives

$$s^* = s_e - \Delta s + \Delta s \cos^2 \theta \left[ 1 + \frac{\Delta s}{\Omega^2 a^2} (T_b - T) \right], \quad (2.31)$$

and

$$u = \frac{\Delta s}{\Omega a} (T_b - T) \cos \theta. \quad (2.32)$$

These are valid outside the critical latitude. The maximum value of the zonal wind occurs at the tropopause at the critical latitude and is given by

$$u_{max} = \frac{\Delta s (T_b - T_t)}{\sqrt{\Omega^2 a^2 + \Delta s (T_b - T_t)}}, \quad (2.33)$$

where  $T_t$  is the tropopause temperature at the critical bounding latitude. Note that for zonal winds that are much less than the rotational velocity of the earth at the equator, (2.33) predicts that the maximum zonal wind varies directly as the pole-to-equator equilibrium entropy difference, and inversely with the earth's rotation rate.

An example of the zonal wind distribution given by (2.29) and (2.31) is shown in Figure 2.12. We have taken a boundary layer entropy difference corresponding to a surface temperature of  $30^\circ C$  at the equator and  $-20^\circ C$  at the pole with a relative humidity of 80% and a uniform tropopause temperature of  $-60^\circ C$ . The latitude of the bounding  $M$  surface at the tropopause in this case is  $21^\circ$ , while the maximum zonal velocity is  $66 \text{ m s}^{-1}$ . Note the absence of any vertical gradient of zonal wind inside the bounding  $M$  surface.

## References

- [1] Emanuel, K. A., 1983a: The Lagrangian parcel dynamics of moist symmetric instability. *J. Atmos. Sci.* **40**, 2368–2376.
- [2] Emanuel, K. A., 1983b: On assessing local conditional symmetric instability from atmospheric soundings. *Mon. Wea. Rev.* **111**, 2016–2033.
- [3] Emanuel, K. A., 1986: An air-sea interaction theory for tropical cyclones. Part I. *J. Atmos. Sci.*, **42**, 1062–1071.
- [4] Emanuel, K.A., 1994: *Atmospheric Convection*. Oxford Univ. Press, New York. 580 pp.
- [5] Emanuel, K. A., 1995: On thermally direct circulations in moist atmospheres. *J. Atmos. Sci.* **52**, 1529–1534.

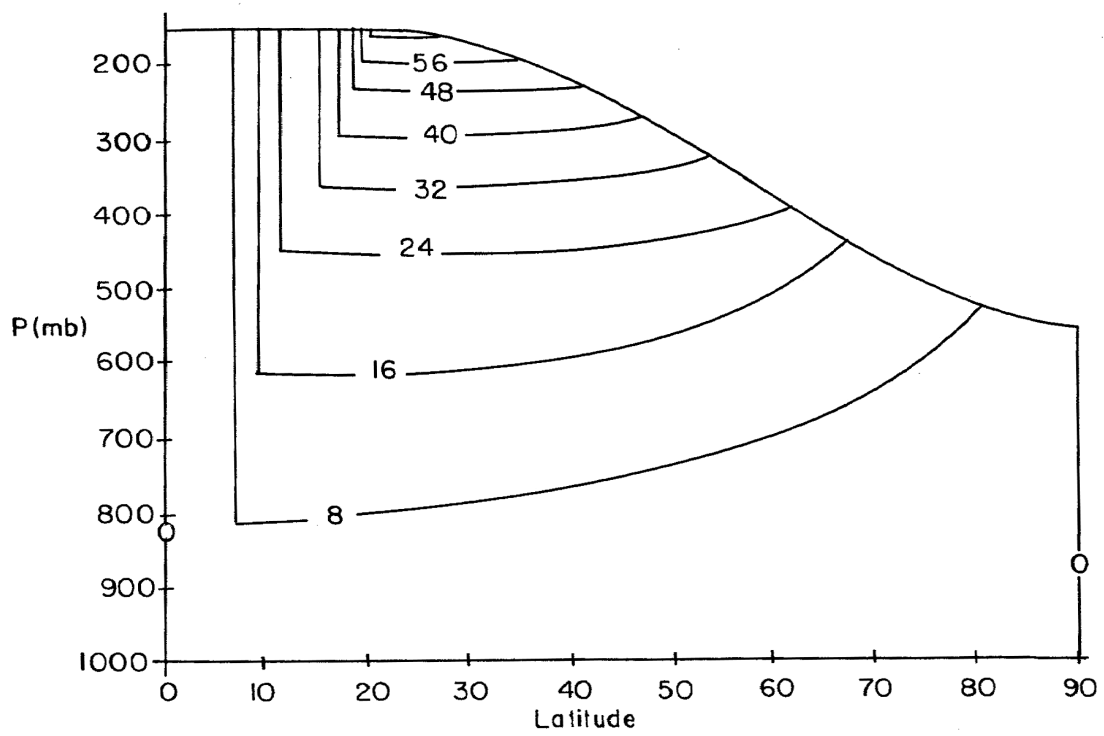


Figure 2.12: Zonal wind in the slantwise-neutral solution given by (2.29) and (2.31).

- [6] Emanuel, K. A., and M. Zivkovic-Rothman, 1999: Development and evaluation of a convection scheme for use in climate models. *J. Atmos. Sci.*, **56**, 1766–1782.
- [7] Held, I. M., and A. Y. Hou, 1980: Nonlinear axially symmetric circulations in a nearly inviscid atmosphere. *J. Atmos. Sci.* **37**, 515–533.
- [8] Lindzen, R. S., and A. Y. Hou, 1988: Hadley circulations for zonally averaged heating centered off the equator. *J. Atmos. Sci.* **45**, 2416–2427.
- [9] Newell et al., 1972: *General Circulation of the Tropical Atmosphere*. MIT Press.
- [10] Oort, A. H., 1983: *Global Atmospheric Circulation Statistics, 1958-1973*. NOAA professional paper #14.
- [11] Plumb, R. A., and A. Y. Hou, 1992: The response of a zonally symmetric atmosphere to subtropical thermal forcing: threshold behavior. *J. Atmos. Sci.* **49**, 1790–1799.
- [12] Rennó, N. O., Emanuel, K. A., and P. H. Stone, 1994: Radiative-convective model with an explicit hydrological cycle, Part I: Formulation and sensitivity to model parameters. *J. Geophys. Res.*, **99**, 14429–14441.
- [13] Robe, F.R., and K.A. Emanuel, 1996: Dependence of tropical convection on radiative forcing. *J. Atmos. Sci.*, **53**, 3265–3275.
- [14] Schneider, E. K., and R. S. Lindzen, 1977: *J. Atmos. Sci.* **34**, 263–279.
- [15] Schneider, E. K., 1977: Axially symmetric steady-state models of the basic state for instability and climate studies. Part I: Nonlinear calculations. *J. Atmos. Sci.* **34**, 280–296.
- [16] Spencer, R.W., and W.D. Braswell, 1997: How dry is the tropical troposphere? Implications for global warming theory. *Bull. Amer. Meteor. Soc.*, **78**, 1097– 1106.